The Journal of Immunology

The Transcription Factor Nrf2 Is a Therapeutic Target against Brain Inflammation

Nadia G. Innamorato, Ana I. Rojo, Ángel J. García-Yagüe, Masayuki Yamamoto, María L. de Ceballos and Antonio Cuadrado

References	This article **cites 36 articles**, 15 of which you can access for free at: http://www.jimmunol.org/content/181/1/680.full#ref-list-1

Why *The JI*? Submit online.

- **Rapid Reviews! 30 days*** from submission to initial decision

- **No Triage!** Every submission reviewed by practicing scientists

- **Fast Publication!** 4 weeks from acceptance to publication

*average

Subscription	Information about subscribing to *The Journal of Immunology* is online at: http://jimmunol.org/subscription
Permissions	Submit copyright permission requests at: http://www.aai.org/About/Publications/JI/copyright.html
Email Alerts	Receive free email-alerts when new articles cite this article. Sign up at: http://jimmunol.org/alerts

The Transcription Factor Nrf2 Is a Therapeutic Target against Brain Inflammation[1]

Nadia G. Innamorato,[*†] **Ana I. Rojo,**[*†] **Ángel J. García-Yagüe,**[*†] **Masayuki Yamamoto,**[‡] **María L. de Ceballos,**[†§] **and Antonio Cuadrado**[2*†]

Because chronic neuroinflammation is a hallmark of neurodegenerative diseases and compromises neuron viability, it is imperative to discover pharmacologic targets to modulate the activation of immune brain cells, the microglia. In this study, we identify the transcription factor Nrf2, guardian of redox homeostasis, as such target in a model of LPS-induced inflammation in mouse hippocampus. Nrf2 knockout mice were hypersensitive to the neuroinflammation induced by LPS, as determined by an increase in F4/80 mRNA and protein, indicative of an increase in microglial cells, and in the inflammation markers inducible NO synthase, IL-6, and TNF-α, compared with the hippocampi of wild-type littermates. The aliphatic isothiocyanate sulforaphane elicited an Nrf2-mediated antioxidant response in the BV2 microglial cell line, determined by flow cytometry of cells incubated with the redox sensitive probe dihydrodichlorofluorescein diacetate, and by the Nrf2-dependent induction of the phase II antioxidant enzyme heme oxygenase-1. Animals treated with sulforaphane displayed a 2–3-fold increase in heme oxygenase-1, a reduced abundance of microglial cells in the hippocampus and an attenuated production of inflammation markers (inducible NO synthase, IL-6, and TNF-α) in response to LPS. Considering that release of reactive oxygen species is a property of activated microglia, we propose a model in which late induction of Nrf2 intervenes in the down-regulation of microglia. This study opens the possibility of targeting Nrf2 in brain as a means to modulate neuroinflammation. *The Journal of Immunology,* **2008, 181: 680–689.**

I n response to multiple noxious stimuli, microglia enters a state of activation that is characterized by the production of chemotactic molecules, metalloproteases, and proinflammatory cytokines (1, 2). Crucial to microglial activation is the production of intracellular and extracellular reactive oxygen species (ROS),[3] mainly through the activation of NADPH oxidase (3). ROS released by microglia contribute to elimination of pathogens and also act as second messengers that activate MAPKs and NFκB and result in further expression of proinflammatory cytokines (4). Persistent ROS and cytokine release from microglia results in peroxidation of lipids and other macromolecules and in activation of apoptotic programs, leading to neuronal death (5). Hence, if microglial activation is not properly controlled, it may lead to a vicious cycle of neuroinflam-

mation that results in neuronal damage. Magnitude and duration of the brain inflammatory response are events that should be modulated by pharmacological means if the proper molecular targets can be found.

The transcription factor Nrf2 is the guardian of redox homeostasis. Under oxidant conditions, it activates a battery of antioxidant and cytoprotective genes that share in common a *cis*-acting enhancer sequence termed antioxidant response element (ARE) that include heme oxygenase-1 (HO-1). Recently, several research groups have reported the relevance of HO-1 in immunomodulation of macrophages, an immune cell type that, like microglia, belongs to the reticuloendothelial system (6). Regarding Nrf2, several studies have demonstrated an essential role of Nrf2 as a key element in modulation of macrophage activation in lung in response to cigarette smoke extracts and to LPS (7, 8). Yet, the relevance of the Nrf2/HO-1 axis in down-regulation of brain inflammation and the design of drugs that could pass through the blood brain barrier to modulate Nrf2 activity are fundamental issues that need to be solved.

The isothiocyanate sulforaphane (SFN) is a natural product found in cruciferous vegetables (9). Although the molecular targets of this molecule are not completely characterized, the best known effect of SFN is to induce Nrf2-dependent gene expression (10). SFN has been used to down-regulate macrophage activation in in vitro models of inflammation (11, 12). Therefore, SFN is an excellent candidate to analyze its capacity to modulate brain inflammation in animal models.

In this study, we report that systemic administration of SFN results in Nrf2-dependent activation of antioxidant phase II enzymes such as HO-1. We show that SFN attenuates microglia-induced inflammation in hippocampus of LPS-treated mice as determined by reduced inducible NO synthase (iNOS) levels and attenuates the production of proinflammatory cytokines IL-6 and TNF-α. Our work paves the way to assess the therapeutic role of

Table I. *Genes, primers, and conditions for semiquantitative PCR amplification*

Gene Product	Forward Primer	Reverse Primer	Fragment Size	Cycles for Linear Range[a]
Nrf2	5′ TGGACGGGACTATTGAAGGCTG 3′	5′ GCCGCCTTTTCAGTAGATGGAGG 3′	179	20
TNF-α	5′ CATCTTCTCAAAATTCGAGTGACAA 3′	5′ TGGGAGTAGACAAGGTACAACCC 3′	175	30
IL-6	5′ GAGGATACCACTCCCAACAGACC 3′	5′ AAGTGCATCATCGTTGTTCATACA 3′	141	30
iNOS	5′ CAAGAGTTTGACCAGAGGACC 3′	5′ TGGAACCACTCGTACTTGGGA 3′	654	30
F4/80	5′ TGCCTTACAACTATGAAGCTCCAC 3′	5′ ACACCACAAGAAGTGCATAGGAA 3′	105	30
HO-1	5′ TGCTCAACATCCAGCTCTTTGA 3′	5′ GCAGAATCTTGCACTTTGTTGCT 3′	120	30
β-actin	5′ TGTTTGAGACCTTCAACACC 3′	5′ CGCTCATTGCCGATAGTGAT 3′	207	21

[a] Linear range was achieved with the indicated number of cycles using a 20-ng cDNA template and the thermal profile described in *Materials and Methods*.

Nrf2 activators in patients with unremitting neuroinflammation which accompanies neurodegenerative diseases.

Materials and Methods

Animals and treatments

Eight-week old male wild-type C57BL/6 mice and Nrf2-knockout littermates (13) were housed at room temperature under a 12 h light-dark cycle. Food and water was provided ad libitum. Animals were cared for according to a protocol approved by the Ethical Committee for Research of the Universidad Autónoma de Madrid following institutional, Spanish and European guidelines (Boletín Oficial del Estado (BOE) of 18 March 1988; and 86/609/EEC, 2003/65/EC European Council Directives). In preliminary experiments several SFN doses (5 to 50 mg/kg administered in one single dose or two doses per day or in daily doses for four days) were tested for brain penetration and HO-1 induction (data not shown). SFN (50 mg/kg) and LPS (1 mg/kg) were prepared in saline solution just before use. These compounds were administered by intraperitoneal injection. Once the experimental schedule was completed, animals were anesthetized with 8 mg/kg ketamine and 1.2 mg/kg xylazine and perfused.

Cell culture, plasmids, and transfections

BV2 microglial cells were cultured in RPMI 1640 medium supplemented with 10% FCS and 80 μg/ml gentamicin in a humidified atmosphere of 5% CO_2 at 37°C with medium changed every 3–4 days. For luciferase assays, BV2 cells were plated onto 24-well plates (75,000 cells/well) and transient transfections were performed with the expression vectors pGL3basic, 3xARE-LUC, pEF-ΔNrf2(DN) (Dr. J. Alam, Department of Molecular Genetics, Ochsner Clinic Foundation, New Orleans, LA), and pcDNA3.1/V5HisB-mNrf2 (Dr. J.D. Hayes, Biomedical Research Centre, Ninewells Hospital and Medical School, University of Dundee, Dundee, U.K.). Cells were transfected with Lipofectamine reagent (Invitrogen) and maintained for 6 h in low-serum medium. Then, cells were treated with 10 μM SFN (LKT Laboratories). After overnight treatment, cells were analyzed for luciferase activity. Luciferase activity was assayed with the Luciferase Assay system (Promega), according to the manufacturer's instructions, and relative light units were measured in a BG1 Optocomp I, GEM Biomedical luminometer (Optocomp).

HPLC determination of SFN

Liver and hippocampus were dissected and rapidly frozen at −80°C until use. Samples were sonicated in 10 volumes (w/v) of methanol. After centrifugation, the supernatant was injected onto a C-18 column (Beckman-Coulter). The solvent system consisted of 20% acetonitrile in water with a linear change to 60% acetonitrile over 10 min, and then maintained at 100% acetonitrile for 2 min to purge the column. Column oven temperature was set at 30°C. The flow rate was 1 ml/min, and 10 μl portions were injected into the column. SFN was detected by UV 254 nm.

Flow cytometry

A FACScan flow cytometer (BD Biosciences) was used to analyze intracellular ROS with the fluorescence probe 2′,7′-dichlorodihydrofluorescein diacetate (H_2DCFDA) (Invitrogen), which passively diffuses into the cell and is cleaved and oxidized to 2′,7′-dichlorofluorescein (band pass 530/25 nm). A total of 400,000 cells were seeded onto 60 mm dishes and grown for 24 h. Then, cells were treated with 10 μM SFN for 16 h, loaded for 1 h with 10 μM H_2DCFDA, and submitted to 1 mg/ml LPS (Sigma-Aldrich) for 2 h. Cells were detached mechanically from the plates, washed once with cold PBS, and analyzed immediately. Three independent samples of 10,000 cells were analyzed for each experimental condition.

Analysis of mRNA levels by semiquantitative RT-PCR and quantitative real-time PCR

Brains were removed and dissected, and total RNA from hippocampus was extracted using TRIzol reagent according to the manufacturer's instructions (Invitrogen). A total of 1 μg of RNA from the different treatments were reverse-transcribed for 75 min at 42°C using 5 U of avian myeloblastosis virus reverse transcriptase (Promega) in the presence of 20 U of RNasin (Promega). Amplification of cDNA was performed in 40 μl of Go *Taq* Flexi Colorless PCR buffer (Promega) containing 0.5 U of Go *Taq* Flexi DNA polymerase (Promega) and 30 pmol of synthetic gene-specific primers. Primer sequences are shown in Table I. To ensure that equal amounts of cDNA were added to the PCR, the *β-actin* housekeeping gene was amplified. After an initial denaturation step for 4 min at 94°C, amplification of each cDNA was performed for the minimum number of cycles that allowed detection of basal mRNA levels in the linear range of each mRNA (data not shown), using a thermal profile of 1 min at 94°C (denaturation), 1 min at 58°C (annealing), and 1 min at 72°C (elongation). The amplified PCR products were resolved in 5% PAGE and stained with ethidium bromide. For real-time PCR analysis, cDNA was synthesized as described before, using equal amounts of RNA. The reaction was performed in 25 μl using the fluorescent dye SYBR Green Master mix (Applied Biosystems) and a mixture of 5 pmol of reverse and forward primers. The primers used were the same as for semiquantitative PCR. Quantification was performed on an ABI PRISM 7900 sequence detection system (Applied Biosystems). PCR cycles proceeded as follows: initial denaturation for 10 min at 95°C, then 40 cycles of denaturation (15 s, 95°C), annealing (30 s, 60°C), and extension (30 s, 60°C). The melting-curve analysis showed the specificity of the amplifications. Threshold cycle, which inversely correlates with the target mRNA level, was measured as the cycle number at which the reporter fluorescent emission appears above the background threshold (data not shown). The relative mRNA levels were estimated by the standard method using housekeeping gene *β-actin* as the reference gene. All of the PCRs were performed in triplicate.

Immunofluorescence and immunohistochemistry

The animals were perfused through the left ventricle with saline solution, followed by 4% paraformaldehyde in 0.1 M phosphate buffer (pH 7.4) for 15 min. The brains were removed and cryoprotected by soaking in 30% sucrose solution in phosphate buffer until they sank. Parallel series of 40-μm thick coronal sections were obtained in a freezing microtome. Sections from control and experimental animals were processed with the same solutions and processing times over the same experimental sessions. Sections were rinsed in 20 mM Tris-HCl (pH 7.6) (TBS). After three washes in TBS, the sections were incubated for 3 h in blocking solution (10% goat or rabbit serum, 0.3% Triton X-100 in TBS), and then for 48 h at 4°C in the following primary Abs: rat anti-F4/80 (1/50; Serotec) and anti-HO-1 (1/100; Stressgen). Sections were rinsed in TBS and washed three times and then incubated with secondary Abs for 45 min: Alexa Fluor 546 goat anti-rabbit or Alexa Fluor 488 goat anti-rat at 1/100 dilution (Invitrogen). Immunoreagents were diluted in 1% goat or rabbit serum and 0.2% Triton X-100 in TBS. The appropriate dilution for each primary Ab was tested and optimized in preliminary experiments. Control sections were run following identical protocols but omitting the primary Ab. Sections were mounted on gelatin-coated slides, air-dried, and finally dehydrated in graded alcohols, cleared in xylene, and cover-slipped. The fluorescence images were captured using appropriate filters in a Leica DMIRE2TCS SP2 confocal microscope (Nussloch). The lasers used were Ar 488 nm for green fluorescence and Ar/HeNe 543 nm for red fluorescence. Lectin immunostaining was performed on floating sections (30 μm). In brief, sections were washed four times in buffer 0.1 M PB containing 0.1% Triton X-100 and 0.2% BSA, treated with 1% H_2O_2 for 15 min to block endogenous peroxidase,
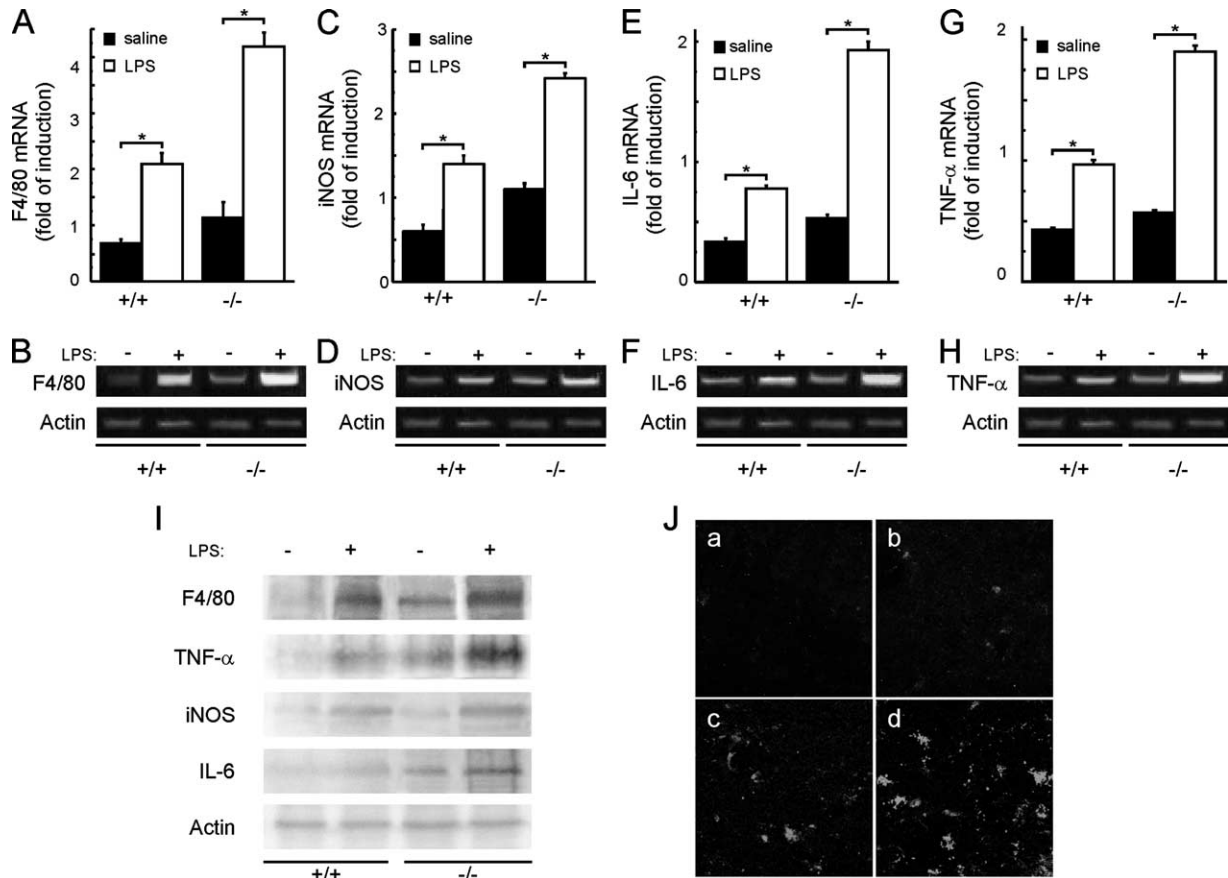
FIGURE 1. Nrf2-deficient mice exhibit enhanced microglial activation in hippocampus. Nrf2 knockout and wild-type littermate mice were injected i.p. with 1 mg/kg LPS. After 7 days, mRNA levels were analyzed for F4/80 (*A* and *B*), iNOS (*C* and *D*), IL-6 (*E* and *F*), and TNF-α (*G* and *H*). *A, C, E,* and *G,* Data from quantitative RT-PCR. Bars represent the mean ± SD from six mice. Asterisks denote statistically significant differences between Nrf2-null (−/−) and wild-type (+/+) groups. *B, D, F,* and *H,* Representative acrylamide gels showing amplification by semiquantitative RT-PCR. *I,* Protein levels of these inflammation markers 6 h after LPS injection. *J,* Immunofluorescence showing F4/80-stained cells in hippocampus CA2 region, 7 days after injection of saline in wild-type (*a*) and Nrf2-null (*b*) mice or 7 days after injection of LPS in wild-type (*c*) and Nrf2-null (*d*) mice.

and rinsed three times in the same buffer. Sections were incubated with biotinylated tomato lectin (1/200; Sigma-Aldrich) 4–6 h at room temperature and overnight at 4°C. Development was conducted by the ABC method (Pierce), and immunoreactivity visualized by 3,3′-diaminobenzidine oxidation as chromogen with nickel enhancement.

Immunoblotting

Hippocampi were removed rapidly and homogenized on ice with lysis buffer (20 mM Tris-HCl (pH 7.5); 137 mM NaCl; 20 mM NaF; 1 mM sodium pyrophosphate; 1 mM Na$_3$VO$_4$; 1% Nonidet P-40; 10% glycerol; 1 mM phenyl methyl sulfonyl fluoride; and 1 μg/ml leupeptin). BV2 cells were lysed in the same buffer. Protein extracts were cleared by centrifugation and 30 μg protein were resolved by SDS-PAGE and transferred to Immobilon-P membranes (Millipore). Blots were analyzed with the appropriate Abs: anti-Nrf2 (1/1000; Santa Cruz Biotechnology); anti-HO-1 (1/2000; Millipore); anti-TNF-α, anti-L6, and anti-iNOS (1/1000; Abcam). Appropriate peroxidase-conjugated secondary Abs (1/10,000) were used to detect the proteins of interest by ECL.

Image analysis, quantification, and statistics

Different band intensities corresponding to immunoblot detection of protein samples and RT-PCR results were quantified using the Image J program (National Institutes of Health, Bethesda, MD). Cytometry experiments were represented using the WinMDI program (Scripps Institute, La Jolla, CA). Real-Time PCR data were analyzed using the Sequence Detector Software SDS 2.0 (Applied Biosystems). The values in graphs correspond to the mean ± SD of at least three samples. Student's *t* test was used to assess differences between groups. Asterisks indicate statistically significant differences with $p < 0.05$.

Results

Nrf2-null mice exhibit exacerbated brain inflammation in response to LPS

We analyzed markers of neuroinflammation in hippocampi of both wild-type and Nrf2 knockout mice submitted to a sublethal dose of LPS (1 mg/kg) administered i.p. As shown in Fig. 1, *A* and *B*, first we determined mRNA levels of F4/80, a gene selectively expressed in microglia/macrophages. One week after the LPS inoculation (see later for a time-course analysis) we found that in wild-type mice the mRNA levels of F4/80 were increased by 2-fold in hippocampus. Interestingly, the Nrf2-deficient mice exhibited a greater sensitivity to LPS, achieving ~4-fold increase in hippocampal F4/80 mRNA levels. The specificity of F4/80 was confirmed by double immunofluorescence with F4/80 and Iba-1 Abs, the latter to unequivocally identify microglia/macrophages. Indeed more that 95% of the stained cells were positive for both Ags (data not shown).

Then, we analyzed the expression of other genes that are indicative of inflammation, such as iNOS (Fig. 1, *C* and *D*), IL-6 (Fig. 1, *E* and *F*), and TNF-α (Fig. 1, *G* and *H*). mRNA levels for these markers were also enhanced in the Nrf2-null mice treated with LPS. The protein levels of these inflammation markers were also increased to a higher extent in the Nrf2-null mice compared with control mice following 6 h after LPS injection, as shown in Fig. 1*I*.
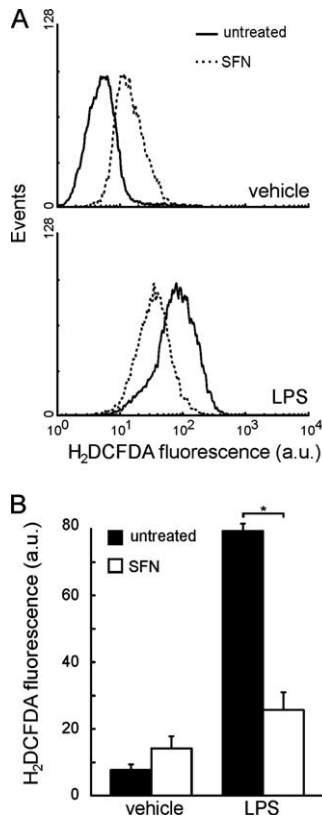
FIGURE 2. SFN modulates the oxidative response in BV2 cells. Cells were treated for 16 h with 10 μM SFN in medium with 0.5% serum. Then, cells were preincubated for 1 h with 10 μM H$_2$DCFDA, treated for 2 h with 1 mg/ml LPS and analyzed by flow cytometry. *A*, Representative samples from three different experiments for each condition are shown. *B*, Quantification of the effect of the SFN in the reduction of ROS levels in microglia. Results are expressed as arbitrary units of H$_2$DCFCA fluorescence. Each value corresponds to the mean $\pm$ SD from three samples of 10,000 cells. Differences between untreated and SFN-treated groups were statistically significant with $p < 0.05$.

Results from microglia-enriched cultures obtained from both mice genotypes submitted to LPS (1 mg/ml) provided similar trends in iNOS, IL-6, and TNF-α mRNA levels as those just commented for hippocampus, thus, suggesting that the inflammation markers were produced, at least in part, by activated microglia (data not shown).

Immunofluorescence analysis of hippocampal sections from the same experimental conditions evidenced an increase in the number of F4/80 immunoreactive cells that was more pronounced in the Nrf2-deficient mice than in control mice (Fig. 1*J*). Therefore there was a correlation between the increase in inflammatory markers and the increase in microglia. Taken together, these results indicate that Nrf2-null mice exhibit exacerbated inflammatory response to LPS that correlates with increased microglial density in hippocampus.

Microglia exhibit redox regulation by Nrf2 in response to LPS

A hallmark of microglial activation is the production of hydrogen peroxide and other ROS in response to pathogens. We used the microglial cell line BV2 to determine whether SFN might modulate ROS production in response to LPS. BV2 cells were serum-starved for 16 h and treated at the same time with SFN. Then, cells were loaded with the ROS sensitive fluorescent probe H$_2$DCFDA, submitted to LPS for 2 h and analyzed by flow cytometry. As shown in Fig. 2, *A* and *B*, LPS promoted a strong oxidation of the fluorophore ($\sim$7-fold). SFN alone induced a small oxidation of this dye ($\sim$2-fold over the basal level) that we ascribe to the tendency of these cells to react against most external stimuli with a respiratory burst. Interestingly, SFN pretreatment significantly attenuated LPS-induced ROS production ($\sim$4-fold). These results indicate that LPS induces an oxidant response in BV2 cells and that SFN significantly attenuates this process.

Several studies have shown that the transcription factor Nrf2 is regulated by SFN in other cell models. To determine whether this isothiocyanate regulates the Nrf2 pathway in microglia, BV2 cells were transfected with a luciferase reporter construct harboring three ARE (ARE-LUC) of the mouse HO-1 gene promoter (*hmox1*). Cells were also cotransfected, as described in Fig. 3, *A*
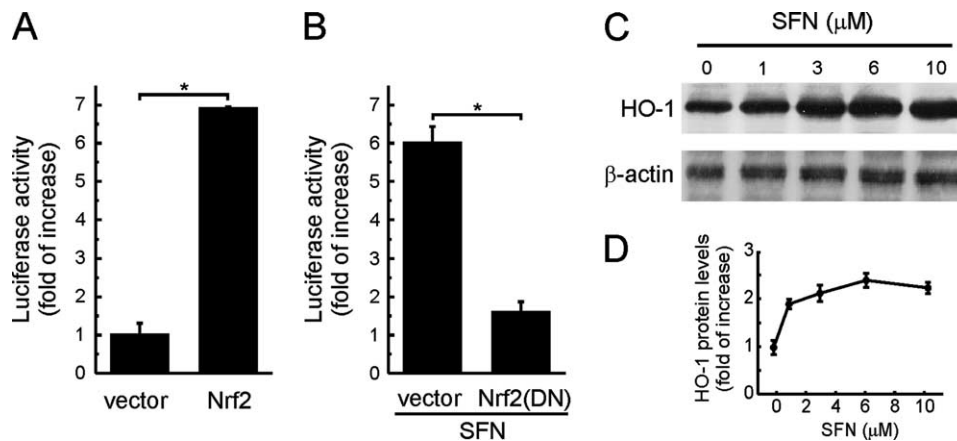

FIGURE 3. The Nrf2 pathway is functional in microglial cells. *A*, BV2 cells were cotransfected with either empty vector or Nrf2 wild-type vector (pcDNA 3.1/V5HisB-mNrf2) and a reporter construct for Nrf2 transactivating activity (ARE-LUC) containing 3 tandem sequences of the mouse *hmox1* ARE. After 24 h, cells were analyzed for luciferase activity. *B*, BV2 cells were cotransfected with either empty vector or expression vector for dominant negative Nrf2 mutant (pEF-ΔNrf2). After 6 h, cells were treated with 10 μM SFN and maintained for 16 h until analysis for luciferase activity. Bars represent the mean $\pm$ SD from three samples. *C*, Representative immunoblot showing HO-1 protein levels in BV2 cells treated with SFN. Cells were serum-starved for 16 h and simultaneously treated with 1–10 μM SFN and analyzed for HO-1 protein levels. *Upper panel*, anti-HO-1 Ab; *lower panel*, anti-β-actin Ab, showing similar protein load per lane. *D*, Quantification of HO-1 protein levels in *C* after normalization by β-actin levels. Similar results were obtained in two additional immunoblots.

FIGURE 4. SFN activates the Nrf2/HO-1 axis in hippocampus. *A*, Representative samples of liver and hippocampus used to determine SFN levels in liver and hippocampus by HPLC 10 min after a single i.p. injection of 50 mg/kg. The arrows indicate the peak identified as SFN by UV absorbance. *B*, Kinetic analysis of SFN levels in liver and hippocampus analyzed as in *A*. Bars indicate mean ± SD of six mice per time point. *C* and *D*, Mice were submitted to one i.p. injection of 50 mg/kg SFN. After 16 h, mRNA (*C*) and protein (*D*) levels were analyzed in the hippocampi of wild-type (+/+) and Nrf2 knockout (−/−) mice. *E*, Quantification of HO-1 protein levels in *F* after normalization by β-actin levels. Similar results were obtained in two additional immunoblots. *F*, Representative immunoblot showing a time-course analysis of HO-1 protein levels in wild-type mice after one i.p. injection of 50 mg/kg SFN.
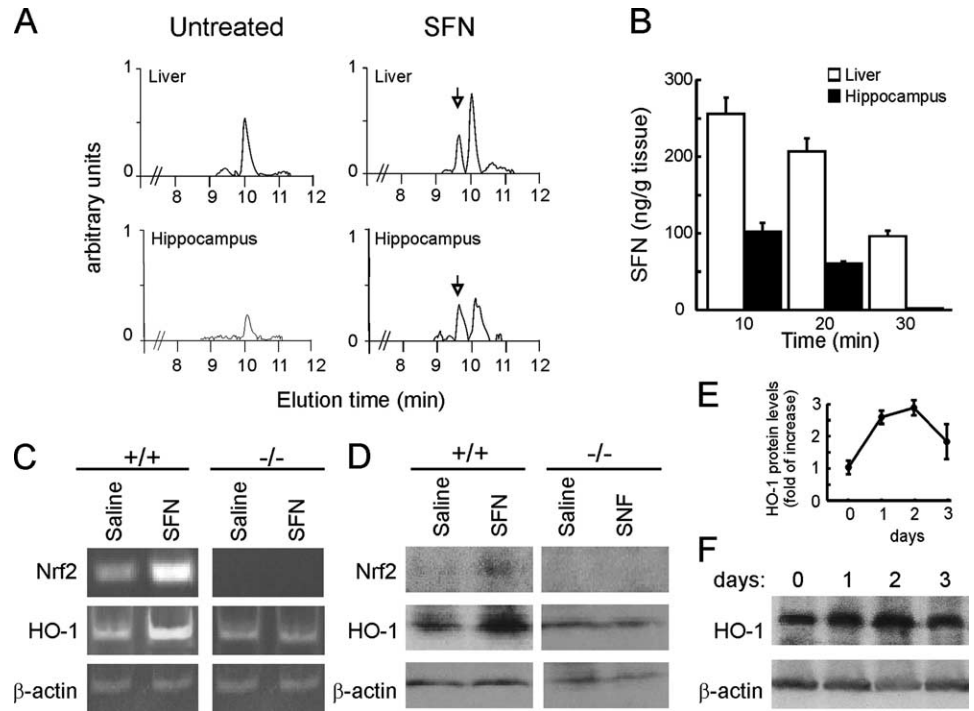
and *B*, with either a control empty vector, or expression vectors for Nrf2 or a dominant negative Nrf2 mutant. Nrf2 overexpression induced a 6-fold increase in ARE activity (Fig. 3*A*). Treatment with SFN for 16 h resulted in a 6-fold increase in ARE activation as well. Moreover, SFN-induced activation of ARE was drastically blocked in cells cotransfected with the Nrf2 dominant negative mutant.

In additional experiments, we analyzed the effect of SFN on HO-1 protein levels. We chose this protein because it is a prototypic antioxidant enzyme, regulated by Nrf2, and it has been implicated in modulation of macrophage activity. BV2 cells were serum-starved for 16 h and stimulated with the indicated concentrations of SFN. As shown in Fig. 3, *C* and *D*, HO-1 protein levels increased 2–3-fold following treatment with 6–10 μM SFN. As it will be commented in *Discussion*, this modest induction is very relevant to achieve a neuroprotective and immunomodulatory effect without compromising cell viability.

Therefore, these genetic and pharmacologic approaches show that microglia has a functionally responsive Nrf2 pathway and that SFN regulates this process.

SFN activates HO-1 expression and attenuates microglial activation in the hippocampus

Encouraged by the observation in Nrf2-null mice that Nrf2 is needed to prevent the LPS-enhanced microglial activation and by the finding that SFN activates the Nrf2 antioxidant response in vitro, we sought to analyze whether SFN might attenuate the microglial response in vivo as well. First, by HPLC analysis (14), we obtained evidence that SFN passes the blood brain barrier. As shown in Fig. 4*A*, untreated mice exhibited an unspecific peak at 10 min elution in both liver and hippocampus extracts. Interestingly, SFN-treated mice (10 min after i.p. injection of 50 mg/kg SFN) exhibited an additional elution peak at 9.5 min that was identified by UV absorbance as SFN. As shown in Fig. 4*B*, in
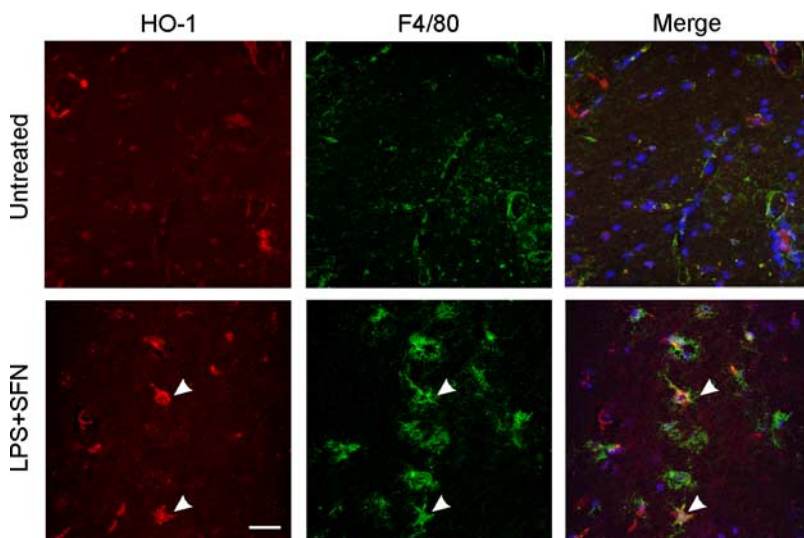

FIGURE 5. Double immunofluorescence with anti-HO-1 (red) and anti-F4/80 (green) Abs showing that a fraction of microglia/macrophages showed increased HO-1 protein levels in response to SFN. Note the reticular and membrane distribution of HO-1. Double immunofluorescence was done in 40-μm thick coronal sections of hippocampi stained with the indicated Abs and counterstained with 4′,6-diamidino-2-phenylindole. *Upper panels*, Control animals injected with saline. *Lower panels*, Mice received one i.p. injection of 1 mg/kg LPS 3 days before analysis, and one i.p. injection of 50 mg/kg SFN, 2 days before analysis, to stimulate HO-1 gene expression. Arrows point microglial cells expressing HO-1. Bar indicates 100 μm.
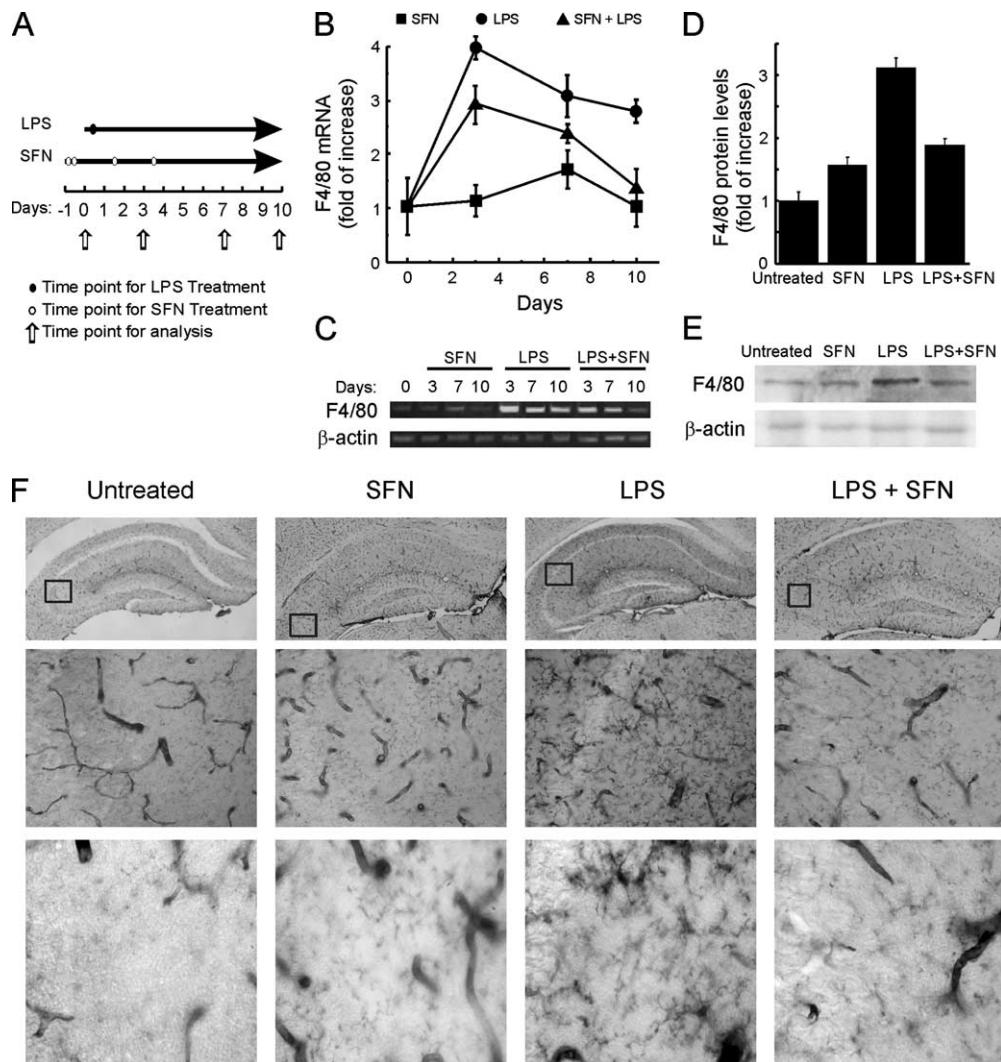
FIGURE 6. SFN attenuates the LPS-induced microglial infiltration to hippocampus. *A,* Experimental protocol of SFN and LPS administration. Mice received two SFN i.p. injections (50 mg/kg) 8 h apart from each other (day -1) and reinforcement doses at days 1 and 3. LPS (1 mg/kg) was injected in a single dose at day 0. *B,* Time-course analysis by real-time PCR of F4/80 mRNA levels in hippocampi of mice submitted to LPS, SFN, or LPS+SFN as indicated in *A*. Values correspond to F4/80 mRNA levels normalized by β-actin mRNA levels in the same extract. Each point is the mean $\pm$ SD from six mice. *C,* Representative acrylamide gel showing F4/80 mRNA levels detected by semiquantitative RT-PCR. *Upper panel,* F4/80 mRNA. *Lower panel,* β-actin mRNA. *D,* Quantification of F4/80 protein levels in *E* after normalization by β-actin levels. Similar results were obtained in two additional immunoblots. *E,* Representative immunoblot showing F4/80 protein levels at day 7 of protocol described in *A*. *F,* Immunohistochemistry on 40-μm coronal sections of hippocampi stained with tomato lectin, which is an effective marker of vessels and microglial cells in rodents. Mice were submitted to the SFN/LPS protocol of *A*, and analyzed at day 7. *Upper panels,* general view of left hippocampus. *Middle panels,* detail of squared regions in *upper panels* showing microglia and roughly similar microvessel density.

both organs maximum SFN levels were observed following 10 min after SFN injection and were still observed after 30 min, although liver levels were consistently much higher that hippocampal levels.

Then, we analyzed whether the amount of SFN that reaches the brain is sufficient to activate Nrf2 signaling. Sixteen hours following one single i.p. injection of 50 mg/kg SFN provoked in hippocampus a 3–4-fold increase in mRNA levels (Fig. 4*C*) and a 2-fold increase in protein levels (Fig. 4*D*) of Nrf2 and HO-1 in wild-type but not in Nrf2-null mice. Furthermore, HO-1 protein levels remained elevated at least 2 days (Fig. 4, *E* and *F*). Nrf2 protein levels seemed to increase less than mRNA levels. This difference is most likely due to the fact that Nrf2 protein and mRNA have different turnover kinetics. In fact, even dissociated from Keap1, Nrf2 has a very short half-life (15).

The induction of the Nrf2/HO-1 axis in hippocampus of SFN-treated mice included but was not limited to microglia. To determine whether the induction of HO-1 expression took place in microglia, we performed immunofluorescence studies on 40-μm thick hippocampus coronal sections of mice submitted to 1 injection of LPS (1 mg/kg; 3 days before animal perfusion) and 1 injection of SFN (50 mg/kg; 1 day before perfusion). These conditions were chosen to optimize microglial activation and HO-1 induction because LPS alone did not substantially increase HO-1 protein levels (data not shown). We could not detect Nrf2 reliably by immunofluorescence because commercially available polyclonal Abs are not specific enough. In fact, they cross-react in immunoblots with several unidentified proteins (16). To circumvent this problem, we analyzed HO-1 protein levels in response to SFN, which should provide an indirect evidence of Nrf2 signal activation. As shown in Fig. 5, double immunofluorescence with anti-F4/80 and anti-HO-1 Abs indicated that a fraction of the cells stained with the F4/80 Ab were also costained with HO-1 Ab representing a microglia/macrophage subpopulation that induces the
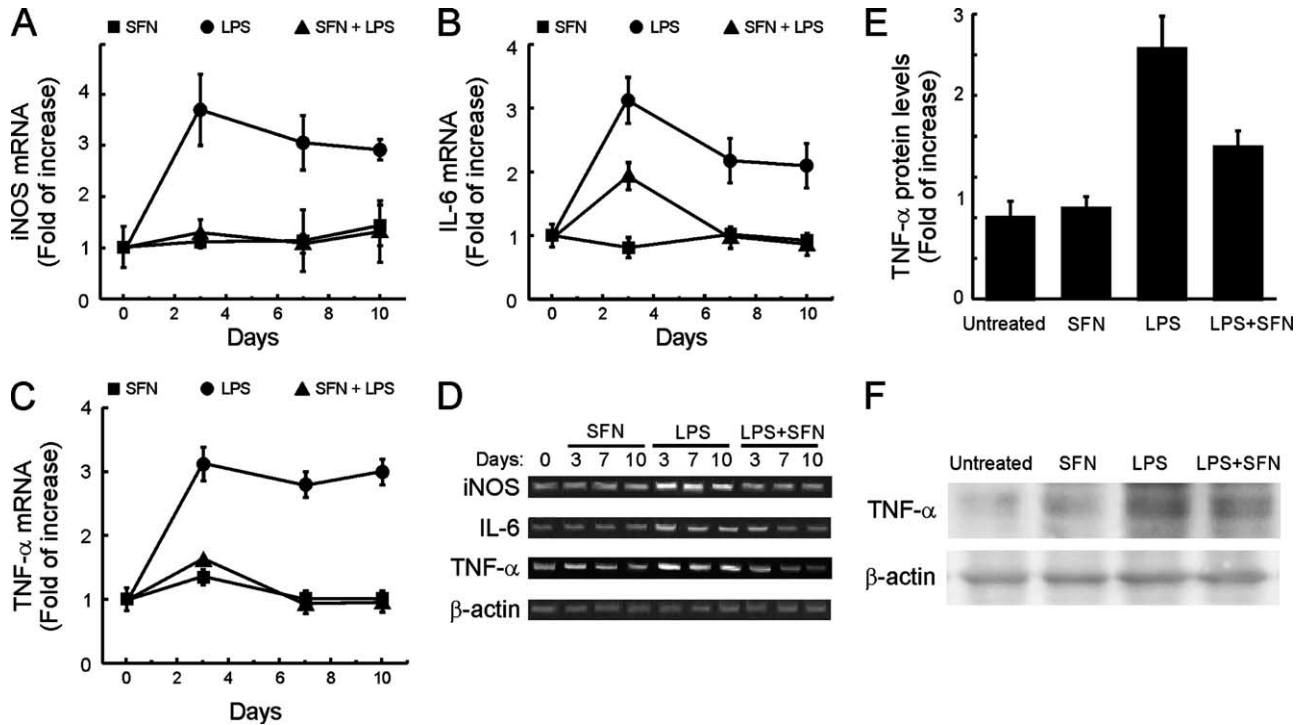
FIGURE 7. SFN attenuates LPS-induced inflammation in hippocampus. Mice were submitted to the SFN/LPS protocol of Fig. 5 and sacrificed at the indicated time points. *A*, *B*, and *C*, Quantification of hippocampal iNOS, IL-6, and TNF-α mRNA levels. Values correspond to iNOS, IL-6, and TNF-α mRNA levels normalized by β-actin mRNA levels in the same extracts. Each point is the mean $\pm$ SD from six mice. *D*, Representative acrylamide gel showing iNOS, IL-6, TNF-α, and β-acting mRNA levels detected by semiquantitative RT-PCR. *E*, Quantification of TNF-α protein levels in *F* after normalization by β-actin levels. Similar results were obtained in two additional immunoblots. *F*, Representative immunoblot showing TNF-α protein levels at day seven.

Nrf2/HO-1 axis in response to SFN. In contrast, we found HO-1 positive cells that were not stained with the F4/80 Ab, indicating that other cell types of the hippocampus are also responsive to SFN.

Several schedules and doses of SFN were tested to achieve a steady increase in hippocampal HO-1 protein levels. SFN did not show evidence of toxicity even at the very high dose of 50 mg/kg. For the purpose of this study and considering that one i.p. injection of 50 mg/kg SFN provided increased HO-1 protein levels for over 2 days (Fig. 4, *E* and *F*), we used the protocol depicted in Fig. 6*A*. This protocol consisted of two i.p. injections of 50 mg/kg at 8-h interval (day -1) and one reinforcement dose at days 1 and 3.

Then, we determined whether SFN might decrease the LPS-induced increase in microglia/macrophages in hippocampus. First, we analyzed the hippocampal mRNA levels of F4/80. As shown in Fig. 6, *B* and *C*, LPS promoted a 4-fold increase of this marker that was maximal after 3 days and was still noticeable at day 10. By contrast, mice submitted to the SFN administration protocol exhibited a lower increase of F4/80 mRNA levels (1.5-fold) following 3 days of the LPS challenge and this increase was not statistically significant after 10 days. Similar results were obtained when we analyzed F4/80 protein levels at day 7. As shown in Fig. 6, *D* and *E*, F4/80 protein levels were about 3-fold higher in the LPS-treated mice but decreased to less than 2-fold in the SFN cotreated mice.

In additional experiments, we stained hippocampal sections with tomato lectin, which recognizes glycoproteins selectively expressed in microglia and endothelium. Microvessel density was similar under the four experimental conditions indicating that these treatments do not produce gross microvascular alter-

ations. Regarding microglia, mice injected with saline or SFN did not display a significant difference in staining with this dye in the areas between vessels (Fig. 6*F*), indicating that there is not an increase in this cell type. By contrast, mice submitted to one i.p. dose of LPS exhibited strong microglial activation in hippocampus even after 7 days. This could be observed by the existence of microglial cells in areas between vessels. On the contrary, mice submitted to the SFN protocol were refractory to the effect of LPS. Therefore, these results indicate that mice submitted to the SFN protocol were protected from LPS-induced microgliosis.

Considering that the Nrf2-knockout mice displayed enhanced production of iNOS, and of proinflammatory cytokines IL-6 and TNF-α in response to LPS (Fig. 1), we sought to investigate whether SFN might also modulate these parameters as well as it did with the F4/80 microglial marker in hippocampus. As shown in Fig. 7, *A* and *D*, hippocampal iNOS mRNA levels reached a maximal 2-fold increase 3 days after the LPS inoculation and then dropped slightly during the following days. By contrast, animals pretreated with SFN according to the protocol in Fig. 6*A* exhibited no iNOS mRNA enhancement at that or later times. These results indicate that SFN was able to completely abrogated LPS-induced increase in this transcript in the animals submitted to SFN, implying that activation of the Nrf2/HO-1 axis provides protection against nitrosative stress.

MRNA levels of proinflammatory cytokines IL-6 (Fig. 7, *B* and *D*) and TNF-α (Figs. 7*C* and 6*D*) induced by LPS administration were also decreased in the SFN-treated mice. In control mice, LPS induced a 2-fold increase in IL-6 mRNA levels at 3 and 7 days, respectively. TNF-α mRNA levels were maximal (3-fold) at 3 days after the LPS injection and the increase was maintained over

the following days. However, mice submitted to SFN were very refractory to the production of these cytokines. In fact, SFN prevented almost completely the LPS-induced increased in mRNA levels of IL-6 and TNF-α. In additional experiments, we analyzed TNF-α protein levels by immunoblot. As shown in Fig. 7, *F* and *E*, a 2-fold increase in TNF-α protein levels was detected after 7 days from the LPS insult. By contrast, the SFN treatment significantly reduced these levels to values slightly higher than those of control and SFN-treated mice.

Discussion

Microglial cells activate a complex response that includes the activation of NADPH oxidase and the subsequent release of extracellular and intracellular ROS, in response to pathogens or neurotoxins. ROS act as second messengers to amplify the inflammatory function of microglia (5) but at the same time they activate the transcription factor Nrf2, which leads to expression of antioxidant genes and restores redox homeostasis (17). We hypothesize that the restoration of redox homeostasis is an essential part in down-modulation of reactive microglia. In Fig. 8, we propose a model on how Nrf2 might participate in a physiological negative loop to bring microglia back to the resting state following its activation. A corollary of this model is that, by activating Nrf2 pharmacologically, it should be possible to anticipate or reinforce the inhibitory events that lead to microglial downregulation and, thus, modulate the pathological neuroinflammatory response that characterizes several neurodegenerative diseases.

Therefore, here we have tested this hypothesis by using a well-established model of neuroinflammation based on i.p. administration of the endotoxin LPS and the analysis of inflammation in hippocampus. We found that Nrf2 knockout mice exhibited both enhanced expression of the microglia marker F4/80 and increased number of microglia/macrophage cells, following LPS administration. The experiments conducted in this study do not allow to discriminate whether this increase resulted from macrophage infiltration, or was a consequence of migration from other brain locations, or proliferation of resident microglial cells. Experiments conducted by Simard et al. (18), using stem cells genetically modified to express the green fluorescence protein, elegantly demonstrated that circulating monocytes are able to infiltrate brain parenchyma and differentiate into microglial cells. In addition, the inflammation markers iNOS, IL-6, and TNF-α were increased compared with wild-type littermates. These observations are consistent with a previous report of Biswal's group (7, 8) who demonstrated that lung macrophages of Nrf2-null mice exhibit an exacerbated inflammatory response to LPS and cigarette smoke extracts. Not all cells that were positive for HO-1 were stained with the F4/80 Ab, suggesting that SFN induced the Nrf2/HO-1 axis in other cell types as well including neurons or astroglia. Considering that astrocytes cooperate in the release of proinflammatory cytokines the attenuation of the inflammatory response by SFN may act in part through the inhibition of astroglial release of cytokines. In fact, other authors have suggested that the Nrf2/HO-1 axis is particularly relevant in astroglia (19).

Numerous evidences generated for the past 2–3 years strongly implicate Heme degradation products CO and biliverdin, generated by HO-1, in immunomodulation of macrophages including microglia in vitro (20–22). Thus, CO inhibits NADPH oxidase (23, 24), the main enzyme responsible for microglial ROS release, and TLR 4, involved in LPS signaling (25).

Based on these observations, it would have seemed logical to use regulators of HO activity to modulate neuroinflammation.
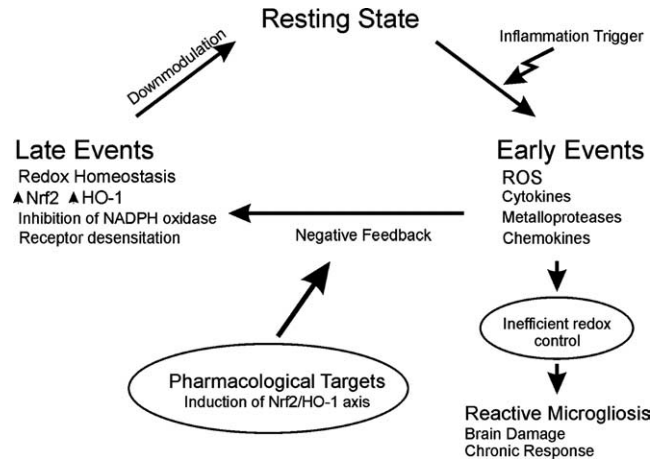

FIGURE 8. Model proposed for modulation of microglia by the Nrf2/HO-1 axis. Pathogenic or neurotoxic insults (LPS) interact with pattern recognition receptors (TLR4) and trigger the early release of NADPH oxidase-mediated ROS and other proinflammatory factors. The increase of intracellular ROS is then detected by Nrf2, guardian of redox homeostasis, which activates a set of antioxidant and anti-xenobiotic genes, including HO-1. This late antioxidant response restores the redox balance, inhibits NADPH oxidase and down-regulates TLR4, driving active microglia back to the resting state. Genetic variability in key antioxidant enzymes, environmental alterations, or just the normal decline of redox homeostasis that occurs with aging leads to inefficient redox control and reduced capacity to down-modulate active microglia. This fact results in microglial activation and brain damage. Pharmacologic action on the Nrf2/HO-1 axis reinforces or restores microglial redox control, strengthens the negative loop, and assists in reduction of neuroinflammation.

However, this possibility has remained elusive because the canonical regulators of HO, Coprotoporphyrin and Sn-protoporphyrin, do not pass the blood brain barrier efficiently (data not shown and 26, 27). Therefore, we have focused on the pharmacological regulation of Nrf2, a transcription factor that activates HO-1 expression and might provide an additional antioxidant protection through the induction of other antioxidant phase II genes.

Initially, we attempted to activate the Nrf2/HO-1 axis with carnosol, a phenolic diterpene extracted from rosemary, which disrupts the Nrf2/Keap1 complex (28). Despite our excellent results in vitro, we could not get a significant activation of Nrf2/HO-1 in vivo. This is most likely due to low bioavailability of phenolic compounds. Therefore, we used the alkaloid isothyocyanate SFN, which according to our present results readily penetrates into the brain after peripheral administration. SFN has been used to down-regulate macrophage activation in in vitro models of inflammation (11, 29), and very recently it has been used in mice to demonstrate a role in modulation of the blood brain barrier permeability in brain microvessels (10).

First, we showed that SFN effectively counteracts LPS-induced ROS in BV2 microglial cells. Next, we analyzed the effect of SFN on HO-1 protein levels in the BV2 microglial cell line and in hippocampus. Maximal 2–3-fold stimulation was observed in both experimental settings. Furthermore, the response was blunted in cells transfected with the dominant negative Nrf2 construct and in Nrf2-null mutant mice, demonstrating the role played by this transcription factor in the SFN effects. Although the increase in HO-1 promoted by SFN may seem small at first glance, it is very relevant to achieve a neuroprotective and immunomodulator effect without compromising cell viability. For the past years, there has been some controversy on whether heme degradation in the brain by

HO-1 prevents or rather contributes to neurodegeneration. Although low levels of CO and biliverdin/bilirubin appear to be neuroprotective, high CO levels may uncouple the mitochondrial respiratory chain and high bilirubin levels, as those found in neonatal jaundice, result in damage to basal ganglia, hippocampus, and cranial nerve nuclei (30, 31). Most importantly, free iron is not efficiently cleared from the brain and contributes to generation of ROS by Fenton reaction (32). In contrast, HO-2 knockout mice display a significant reduction of brain bilirubin and the neurons of these animals are more sensitive to H_2O_2 than matched control wild-type littermates, suggesting a role of bilirubin in neuroprotection against oxidative stress (33). Oxidant scavenging by bilirubin implies its spontaneous conversion back to biliverdin and its recycling through catalysis by biliverdin reductase. According to Sedlak and Snyder (33) in this cycle nanomolar concentrations of bilirubin counteract the oxidative effect of micromolar concentrations of H_2O_2. Bilirubin is also an excellent scavenger for endogenous NO and prevents peroxinitrite formation (34, 35). Therefore, nowadays it is widely accepted that a moderate activation of heme catabolism is neuroprotective (36). For this reason, the modest 2–3-fold increase in HO-1 protein levels reported with our protocol may be within the window of therapeutic benefit.

In vivo administration of SFN was able to decrease microglial activation and the up-regulation of inflammatory markers following endotoxin injection. The effect of SFN on the kinetic response to LPS was slightly different for the inflammation parameters tested in this study. Although iNOS and TNF-α responses were totally abrogated by SFN at 3 days, the F4/80 and IL-6 rise was only partially inhibited at that time point. We do not have a fully satisfactory explanation for these observations but we speculate that part of the proinflammatory markers studied may derive from different cell types including astroglia. Moreover, as shown in Fig. 5, F4/80 microglia included both HO-1-expressing and HO-1-negative subpopulations, suggesting the existence of microglia subsets with different sensitivity to SFN. In any case, SFN significantly reduced the consequences of LPS at 3 days postinjection and totally abrogated the inflammatory response at longer times.

To endorse this kind of treatment into the clinic, a critical issue that needs to be addressed in the near future is the determination of dose and dosing protocol of SFN or other phase II inducers that might have a therapeutic use. In this study, we chose the inoculation of 50 mg/kg because mice did not show evidence of toxicity, even at this very high dose. However, lower doses may be useful too. A recently published study by Zhao et al. (10) show Nrf2 activation in brain by 5 mg/kg SFN. We have corroborated that this dose activates HO-1 expression in brain equally or even better than in liver (data not shown).

In summary, we have shown that pharmacological up-regulation of the transcription factor Nrf2, the guardian of redox homeostasis, which enhances HO-1 activity, is a feasible strategy to modulate an acute inflammatory response in the brain. Moreover, our results open the possibility that this therapeutic intervention might be useful in treatment of pathologies that involve chronic inflammation, such as that observed in some neurodegenerative diseases.

Acknowledgements

Disclosures

The authors have no financial conflict of interest.

References

1. Nimmerjahn, A., F. Kirchhoff, and F. Helmchen. 2005. Resting microglial cells are highly dynamic surveillants of brain parenchyma in vivo. *Science* 308: 1314–1318.
2. Block, M. L., and J. S. Hong. 2005. Microglia and inflammation-mediated neurodegeneration: multiple triggers with a common mechanism. *Prog. Neurobiol.* 76: 77–98.
3. Babior, B. M. 2000. Phagocytes and oxidative stress. *Am. J. Med.* 109: 33–44.
4. Pawate, S., Q. Shen, F. Fan, and N. R. Bhat. 2004. Redox regulation of glial inflammatory response to lipopolysaccharide and interferon-γ. *J. Neurosci. Res.* 77: 540–551.
5. Block, M. L., L. Zecca, and J. S. Hong. 2007. Microglia-mediated neurotoxicity: uncovering the molecular mechanisms. *Nat. Rev.* 8: 57–69.
6. Kapturczak, M. H., C. Wasserfall, T. Brusko, M. Campbell-Thompson, T. M. Ellis, M. A. Atkinson, and A. Agarwal. 2004. Heme oxygenase-1 modulates early inflammatory responses: evidence from the heme oxygenase-1-deficient mouse. *Am. J. Pathol.* 165: 1045–1053.
7. Thimmulappa, R. K., H. Lee, T. Rangasamy, S. P. Reddy, M. Yamamoto, T. W. Kensler, and S. Biswal. 2006. Nrf2 is a critical regulator of the innate immune response and survival during experimental sepsis. *J. Clin. Invest.* 116: 984–995.
8. Rangasamy, T., C. Y. Cho, R. K. Thimmulappa, L. Zhen, S. S. Srisuma, T. W. Kensler, M. Yamamoto, I. Petrache, R. M. Tuder, and S. Biswal. 2004. Genetic ablation of Nrf2 enhances susceptibility to cigarette smoke-induced emphysema in mice. *J. Clin. Invest.* 114: 1248–1259.
9. Fahey, J. W., Y. Zhang, and P. Talalay. 1997. Broccoli sprouts: an exceptionally rich source of inducers of enzymes that protect against chemical carcinogens. *Proc. Natl. Acad. Sci. USA* 94: 10367–10372.
10. Zhao, J., A. N. Moore, J. B. Redell, and P. K. Dash. 2007. Enhancing expression of Nrf2-driven genes protects the blood brain barrier after brain injury. *J. Neurosci.* 27: 10240–10248.
11. Killeen, M. E., J. A. Englert, D. B. Stolz, M. Song, Y. Han, R. L. Delude, J. A. Kellum, and M. P. Fink. 2006. The phase 2 enzyme inducers ethacrynic acid, DL-sulforaphane, and oltipraz inhibit lipopolysaccharide-induced high-mobility group box 1 secretion by RAW 264.7 cells. *J. Pharmacol. Exp. Ther.* 316: 1070–1079.
12. Heiss, E., and C. Gerhauser. 2005. Time-dependent modulation of thioredoxin reductase activity might contribute to sulforaphane-mediated inhibition of NF-kappaB binding to DNA. *Antioxid. Redox Signal.* 7: 1601–1611.
13. Itoh, K., T. Chiba, S. Takahashi, T. Ishii, K. Igarashi, Y. Katoh, T. Oyake, N. Hayashi, K. Satoh, I. Hatayama, et al. 1997. An Nrf2/small Maf heterodimer mediates the induction of phase II detoxifying enzyme genes through antioxidant response elements. *Biochem. Biophys. Res. Commun.* 236: 313–322.
14. Liang, H., Q. Yuan, and Q. Xiao. 2005. Purification of sulforaphane from Brassica oleracea seed meal using low-pressure column chromatography. *J. Chromatogr. B Analyt. Technol. Biomed. Life Sci.* 828: 91–96.
15. McMahon, M., N. Thomas, K. Itoh, M. Yamamoto, and J. D. Hayes. 2004. Redox-regulated turnover of Nrf2 is determined by at least two separate protein domains, the redox-sensitive Neh2 degron and the redox-insensitive Neh6 degron. *J. Biol. Chem.* 279: 31556–31567.
16. Nguyen, T., P. J. Sherratt, P. Nioi, C. S. Yang, and C. B. Pickett. 2005. Nrf2 controls constitutive and inducible expression of ARE-driven genes through a dynamic pathway involving nucleocytoplasmic shuttling by Keap1. *J. Biol. Chem.* 280: 32485–32492.
17. Kraft, A. D., J. M. Lee, D. A. Johnson, Y. W. Kan, and J. A. Johnson. 2006. Neuronal sensitivity to kainic acid is dependent on the Nrf2-mediated actions of the antioxidant response element. *J. Neurochem.* 98: 1852–1865.
18. Simard, A. R., and S. Rivest. 2004. Bone marrow stem cells have the ability to populate the entire central nervous system into fully differentiated parenchymal microglia. *FASEB J.* 18: 998–1000.
19. Kraft, A. D., D. A. Johnson, and J. A. Johnson. 2004. Nuclear factor E2-related factor 2-dependent antioxidant response element activation by tert-butylhydroquinone and sulforaphane occurring preferentially in astrocytes conditions neurons against oxidative insult. *J. Neurosci.* 24: 1101–1112.
20. Lee, S., and K. Suk. 2007. Heme oxygenase-1 mediates cytoprotective effects of immunostimulation in microglia. *Biochem. Pharmacol.* 74: 723–729.
21. Min, K. J., M. S. Yang, S. U. Kim, I. Jou, and E. H. Joe. 2006. Astrocytes induce hemeoxygenase-1 expression in microglia: a feasible mechanism for preventing excessive brain inflammation. *J. Neurosci.* 26: 1880–1887.
22. Guo, G., and N. R. Bhat. 2006. Hypoxia/reoxygenation differentially modulates NF-κB activation and iNOS expression in astrocytes and microglia. *Antioxid. Redox Signal.* 8: 911–918.
23. Taille, C., J. El-Benna, S. Lanone, J. Boczkowski, and R. Motterlini. 2005. Mitochondrial respiratory chain and NAD(P)H oxidase are targets for the antiproliferative effect of carbon monoxide in human airway smooth muscle. *J. Biol. Chem.* 280: 25350–25360.
24. Wang, X., Y. Wang, H. P. Kim, K. Nakahira, S. W. Ryter, and A. M. Choi. 2007. Carbon monoxide protects against hyperoxia-induced endothelial cell apoptosis by inhibiting reactive oxygen species formation. *J. Biol. Chem.* 282: 1718–1726.
25. Nakahira, K., H. P. Kim, X. H. Geng, A. Nakao, X. Wang, N. Murase, P. F. Drain, X. Wang, M. Sasidhar, E. G. Nabel, et al. 2006. Carbon monoxide differentially inhibits TLR signaling pathways by regulating ROS-induced trafficking of TLRs to lipid rafts. *J. Exp. Med.* 203: 2377–2389.

26. Marinissen, M. J., T. Tanos, M. Bolos, M. R. de Sagarra, O. A. Coso, and A. Cuadrado. 2006. Inhibition of heme oxygenase-1 interferes with the transforming activity of the Kaposi sarcoma herpesvirus-encoded G protein-coupled receptor. *J. Biol. Chem.* 281: 11332–11346.

27. Li, M., S. Peterson, D. Husney, M. Inaba, K. Guo, E. Terada, T. Morita, K. Patil, A. Kappas, S. Ikehara, and N. G. Abraham. 2007. Interdiction of the diabetic state in NOD mice by sustained induction of heme oxygenase: possible role of carbon monoxide and bilirubin. *Antioxid. Redox Signal.* 9: 855–863.

28. Martin, D., A. I. Rojo, M. Salinas, R. Diaz, G. Gallardo, J. Alam, C. M. De Galarreta, and A. Cuadrado. 2004. Regulation of heme oxygenase-1 expression through the phosphatidylinositol 3-kinase/Akt pathway and the Nrf2 transcription factor in response to the antioxidant phytochemical carnosol. *J. Biol. Chem.* 279: 8919–8929.

29. Heiss, E., C. Herhaus, K. Klimo, H. Bartsch, and C. Gerhauser. 2001. Nuclear factor κB is a molecular target for sulforaphane-mediated anti-inflammatory mechanisms. *J. Biol. Chem.* 276: 32008–32015.

30. Kapitulnik, J. 2004. Bilirubin: an endogenous product of heme degradation with both cytotoxic and cytoprotective properties. *Mol. Pharmacol.* 66: 773–779.

31. Dennery, P. A., D. S. Seidman, and D. K. Stevenson. 2001. Neonatal hyperbilirubinemia. *N. Engl. J. Med.* 344: 581–590.

32. Lee, D. W., J. K. Andersen, and D. Kaur. 2006. Iron dysregulation and neurodegeneration: the molecular connection. *Mol. Interv.* 6: 89–97.

33. Sedlak, T. W., and S. H. Snyder. 2006. Messenger molecules and cell death: therapeutic implications. *J. Am. Med. Assoc.* 295: 81–89.

34. Mancuso, C., A. Bonsignore, E. Di Stasio, A. Mordente, and R. Motterlini. 2003. Bilirubin and S-nitrosothiols interaction: evidence for a possible role of bilirubin as a scavenger of nitric oxide. *Biochem. Pharmacol.* 66: 2355–2363.

35. Kaur, H., M. N. Hughes, C. J. Green, P. Naughton, R. Foresti, and R. Motterlini. 2003. Interaction of bilirubin and biliverdin with reactive nitrogen species. *FEBS Lett.* 543: 113–119.

36. Cuadrado, A., and A. I. Rojo. 2008. Heme oxygensae-1 as a therapeutic target in neurodegenerative diseases and brain infection. *Curr. Pharm. Design* 14: 429–442.